ELSEVIER

European Journal of Pharmaceutics and Biopharmaceutics 49 (2000) 47–58

European Journal of Pharmaceutics and Biopharmaceutics

www.elsevier.com/locate/ejphabio

Research paper

Modeling of drug release from swellable polymers

Christopher S. Brazel[1], Nikolaos A. Peppas*

Biomaterials and Drug Delivery Laboratories, School of Chemical Engineering, Purdue University, West Lafayette, IN, USA

Received 10 September 1998; accepted in revised form 17 August 1999

Abstract

The water swelling and drug diffusion from initially hydrophilic, glassy polymer matrices were modeled using concentration-dependent diffusion equations for water and drug. The transport equation for water incorporated a relaxation-dependent mechanism. These equations were solved with an appropriate boundary condition incorporating a relaxation-dependent Deborah number. Experimental results from drug release from PVA and PHEMA samples were used to determine the validity of the model.

Keywords: Relaxation; Swellable systems; Drug release; Poly(vinyl alcohol); Poly(2-hydroxyethyl methacrylate)

1. Introduction

There have been many attempts to model the process of solvent penetration and subsequent solute release in polymeric materials, with many valuable contributions to the understanding of the mechanisms behind these processes [1–5]. However, a majority of these models are either too general or require such a significant amount of knowledge of system parameters and complex differential expressions that they have not been successfully used in the development of pharmaceutical formulations.

In this work, a novel parametric model was used to predict the time-dependence of solvent penetration and drug release based on the definitions of dimensionless groups important in the swelling process [6–10]. The results give insight into how polymer carrier characteristics can be adjusted to design a swelling-controlled release device. Though specific for the polymer and drug systems investigated here, results are applicable in general to any similar system.

Water uptake and drug delivery from swelling-controlled release systems can be described sufficiently by two dimensionless parameters for many polymer/solvent systems. The diffusional Deborah number, *De*, relates water motion to the rate of polymer relaxation, and the Swelling Interface number, *Sw*, measures water penetration into a network relative to diffusion of a dispersed drug out of the polymer. These parameters are sensitive to both polymer and drug properties.

The diffusional Deborah number is expressed as a ratio between the characteristics polymer relaxation time and a characteristic diffusion time:

$$De = \frac{\lambda}{\theta} = \frac{\lambda D_{1,2}}{(\delta(t))^2} = \frac{\text{Relaxation time}}{\text{Diffusion of solvent}} \quad (1)$$

where λ is the characteristic relaxation time for the polymer when subjected to swelling stresses, and θ is the characteristic water diffusion time into a swelling sample defined as the square of the diffusional distance (e.g., the half-thickness of a thin disc sample, as used in this work) divided by the diffusion coefficient of water in the polymer $\left(\delta^2/D_{1,2}\right)$. If the swelling process is dominated by either the relaxation time ($De \gg 1$) or water diffusion ($De \ll 1$), the time-dependence is Fickian. However, if *De* is on the order of 1, the two processes will occur on the same time scale, leading to anomalous transport behavior.

The Swelling Interface number, *Sw*, is important in describing the balance between solvent penetration and drug release.

$$Sw = \frac{\upsilon\delta_r}{D_{3,21}} = \frac{\text{Solvent motion}}{\text{Solute diffusion}} \quad (2)$$

Here, υ is the velocity of the moving glassy/rubbery front, δ is the thickness of the swollen gel layer, and $D_{3,21}$ is the diffusion coefficient of drug in the polymer. *Sw* is sensitive to both the polymer structure (as it affects water uptake) and drug properties through the solute diffusion coefficient. When *Sw* is significantly greater or smaller than 1, either

* Corresponding author. Biomaterials and Drug Delivery Laboratories, School of Chemical Engineering, Purdue University, West Lafayette, IN 47907-1283, USA. Tel.: +1-765-494-7944; fax: +1-765-494-0805.

E-mail address: peppas@ecn.purdue.edu (N.A. Peppas)

[1] Present address: Department of Chemical Engineering, University of Alabama, Box 870203, Tuscaloosa, AL 35487-0203, USA.

0939-6411/00/$ - see front matter
PII: S0939-6411(99)00058-2

water penetration or drug diffusion will control the release pattern, and the time dependence will be Fickian; however, when *Sw* is on the order of 1, anomalous behavior prevails.

Both dimensionless numbers, *De* and *Sw*, have been shown to vary during the swelling process, so either the initial ($t = 0$) or equilibrium ($t = \infty$) values of *Sw* and *De* were determined for experimental results in the present work.

A variety of methods have been used to model non-Fickian behavior associated with solvent uptake in polymers. Time- or position- dependent diffusion coefficients [2] have been used to account for the sharp change in solvent diffusivity across a swelling front between glassy and rubbery regions in a polymer. Irreversible thermodynamic principles have also been applied to dynamic penetrant uptake in polymer systems, based on a thermodynamic driving force related to water activity. Other modeling efforts have focused on changes in water behavior or the time-dependent viscoelastic relaxation of the polymer as it swells.

In the simplest manner, the time dependent swelling of a polymer has been generally described [11] by

$$\frac{M_t}{M_\infty} = kt^n \tag{3}$$

Eq. (3) is termed the power law model, with n being the diffusional exponent. In this equation M_t/M_∞ represents the fractional uptake of solvent (or release of a solute) normalized with respect to the equilibrium conditions. The variables k and n are constants which can be related to diffusion coefficients and the specific transport mechanism. This equation is used to account for the coupled effects of Fickian diffusion and viscoelastic relaxation in polymer systems. Eq. (3) has been used frequently in the literature, due to its utility in describing the relative importance of Fickian ($n = 0.5$) and Case II ($n = 1.0$) transport in anomalous diffusion. This equation is also capable of predicting Super Case II transport, where $n > 1.0$.

Transport in swelling systems can be described by Fick's Law, with diffusion dependent on concentration gradients. Starting with Fick's Law for diffusion from a plane surface, with a position-dependent diffusion coefficient,

$$\frac{\partial c}{\partial t} = \frac{\partial}{\partial x}\left(D\frac{\partial c}{\partial x}\right) \tag{4}$$

with boundary and initial conditions given below.

$$at\ t = 0,\ c(x,t) = c_0 \tag{5}$$

$$at\ x = \delta(t),\ c = c_b \tag{6}$$

$$at\ x = 0,\ \partial c/\partial x = 0 \tag{7}$$

Here, x is the axial coordinate through which diffusion occurs, c_0 is the initial solute concentration, assumed to be uniform across the sample, and $\delta(t)$ represents the distance from the center of the sample to the surface, which increases with time due to polymer swelling. c_b represents the bulk concentration at the surface of the polymer, usually treated as zero under perfect sink conditions. This equation has been solved to give:

$$\frac{M_t}{M_\infty} = 4\left[\frac{Dt}{\ell^2}\right]^{1/2}\left[\frac{1}{\pi^{1/2}} + 2\sum_{n=1}^{x}(-1)^n \mathrm{ierfc}\left(\frac{n\ell}{2\sqrt{Dt}}\right)\right] \tag{8}$$

which, for short times reduces to:

$$\frac{M_t}{M_\infty} = 4\left[\frac{Dt}{\pi\ell^2}\right]^{1/2} \tag{9}$$

Eq. (9) therefore leads to the square root of time dependence observed in Fickian diffusion. However, the viscoelastic properties of polymers makes modeling transport in polymeric systems especially difficult. Several attempts have been made to model penetrant and solute diffusion in polymers, taking into account the viscoelastic response of the polymer during swelling.

Hopfenberg and Frisch [12] also approached the problem by separating stress relaxation terms from diffusive flux:

$$M_t = M_{\infty,F}\left[1 - \frac{6}{\pi^2}\sum_{n=1}^{x}\frac{1}{n^2}\exp(-n^2k_Ft)\right] + \sum_{i}^{k} M_{\infty,i}[1 - \exp(-k_it)] \tag{10}$$

where $M_{\infty,F}$ is the equilibrium amount of sorption in the polymer before relaxation, k_F is a diffusional rate constant, $M_{\infty,i}$ represents the amount of penetrant uptake during the ith relaxation process, and k_i is the corresponding relaxation rate constant. Therefore, this model explicitly separated the diffusional and relaxation characteristics of penetrant uptake. This was shown to fit experimental data, but many fitting parameters were necessary and it required information about a spectrum of relaxation processes.

Recently, there has been serious interest in modeling drug transport. Petropoulos et al. [3] devised a rigorous model to treat release of solutes from swelling polymeric matrices. The primary thrust of this work was the development of expressions for the diffusion coefficient of penetrant in the polymer and solute as functions of time, as related through the volume fraction of water absorbed into a hydrogel during the swelling process. This model, though capable of predicting solute release, required several fitting parameters which were not necessarily based on phenomenological properties. Vrentas et al. [9] introduced a diffusional Deborah number to characterize sorptive transport in polymer/solvent systems. The diffusional Deborah number was found to give a good indication of the type of transport in a polymer-penetrant system; for Deborah numbers on the order of 1, where characteristic diffusional and relaxational processes occurred on similar time scales, viscoelastic, or anomalous, diffusion was observed. Wu and Peppas [6] developed a mathematical model for anomalous transport in polymers using linear irreversible thermodynamics and a Maxwell model to describe the viscoelastic properties of the

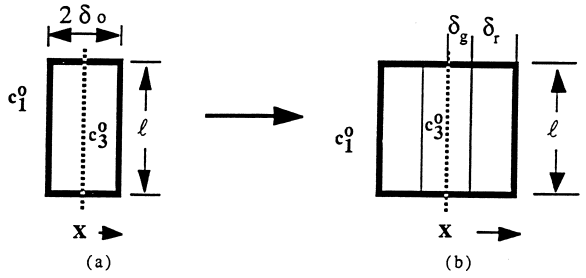

Fig. 1. Schematic of swelling-controlled release problem, as simplified for mathematical analysis. The problem geometry is a thin slab (the sample width in the diagram is exaggerated). The initially dry sample (a) undergoes swelling from the lateral surfaces, leading to glassy and rubbery regions separated by a sharp front (b).

polymer. The transition from Case II to Fickian diffusion was seen to be a strong function of an integral sorption Deborah number.

2. Mathematical definition of the swelling-controlled release problem

A mathematical model was used to relate system parameters to dynamic penetrant uptake and subsequent solute diffusion. In the following analysis, subscripts were used to designate the three components in the system: 1, solvent (water); 2, polymer; and 3, drug. A physical representation of the problem is depicted in Fig. 1.

An initially glassy polymer with thickness, $2\delta_0$, and an exposed surface of length, ℓ, was brought into contact with water at concentration c_1^0 (pure water) at time zero of the process. The water concentration was assumed to remain constant during the release experiment (i.e. a perfect sink assumption was made). Using slab geometry, water diffusion occurred only in the x-direction from the two lateral surfaces (at $x = \pm\delta$). For such geometries with aspect ratios ($\ell/2\delta$) greater than 10, it has been shown that edge effects could be ignored [12] and that the problem can be approached as a one dimensional process. The initial drug concentration in the system, c_3^0, was assumed to be dispersed evenly across the sample. During the swelling and release process, the penetrant (water) diffused into the polymer network through the exposed surfaces, and caused a depression in the glass transition temperature, eventually reaching a high enough concentration to cause the polymer region to swell and become rubbery. Subsequently, the outer edges of the gel expanded outward from the center line of the sample, as a sharp front between rubbery and glassy regions moved towards the center of the sample. The imbedded solute dissolved as water penetrated the sample, and diffused across the gel layer, $\delta_r(t)$.

As depicted in Fig. 2, the solvent and solute concentrations were expected to follow certain general trends. In the glassy region, there were small solvent concentrations due to the pore diffusion through the free volume of the polymer, but this concentration was very small compared to concentrations in the rubbery region. There was a partitioning effect between the glassy and rubbery regions, and the solvent concentration at this boundary (immediately on the rubbery side) was assumed to remain constant during the swelling process at c_1^*. In the rubbery region, there were two sections where polymer relaxation was still occurring and another area close to the surface of the gel which had reached an equilibrium state. Outside of the gel, the free solution concentration, c_1^0, was assumed to remain constant. In Fig. 2b, the solute concentration was assumed to remain constant at c_3^0 until the glassy/rubbery interface reached the drug. In the gel layer, the solute concentration decreased between the swelling front and the polymer surface, with the existence of a diffusion layer as was commonly observed in the outermost section. Moving boundaries were incorporated into the model for the rubbery/glassy interface; however, the sample was assumed to remain at a constant thickness, which was an accurate assumption for systems which swell only minimally.

3. Development of a mathematical model for solvent transport

Mathematically, the swelling-controlled release problem was described by Eq. (11). Beginning with a Fickian expression for one-dimensional concentration-dependent diffusion

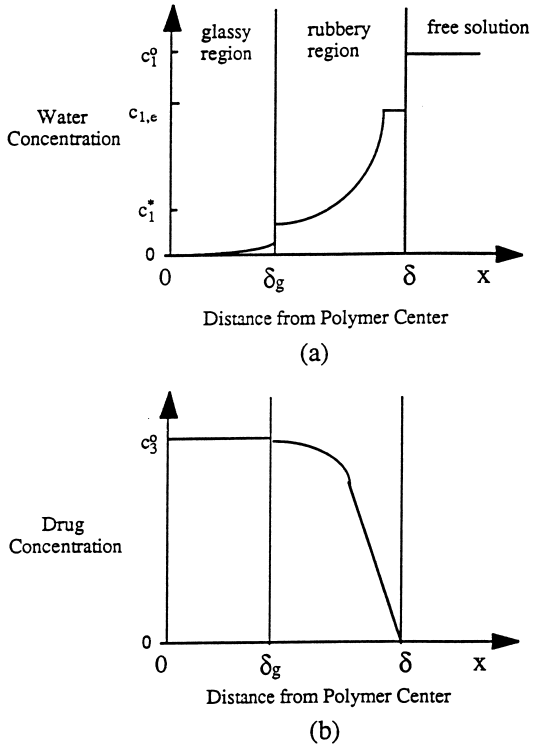

Fig. 2. Theoretical concentration profiles of solvent (a) and solute (b) during the swelling-controlled release process, at a time, t, where the glassy/rubbery front still exists.

of water into a hydrogel, and including a term representing the polymer relaxation rate through the front velocity [13], the concentration of water in the gel was found as a function of time and position.

$$\frac{\partial c_1}{\partial t} = \frac{\partial}{\partial x}\left(D_{1,2}\frac{\partial c_1}{\partial x} - \upsilon c_1\right) \tag{11}$$

The dependence of the diffusion coefficient on concentration was taken as given by Fujita [13]:

$$D_{1,2} = D_1^0 \exp\left[-\beta_1\left(1 - \frac{c_1}{c_{1e}}\right)\right] \tag{12}$$

The diffusivity of water was significantly different between the glassy and rubbery regions. The limit of this equation as the concentration of water reached its equilibrium value in the hydrogel was the diffusion coefficient of water through the swollen gel, D_1^0. Here, β_1 is a material constant derived from free volume theory with approximate values between 2 and 7, while c_1/c_{1e} represented the water concentration normalized with respect to the equilibrium concentration.

The swelling front velocity, υ, being equivalent to $d\delta_g/dt$, was the change in front position over a differential time, δ_g being the distance from the center of the sample to the swelling front. The value of δ_g could be determined, since the solvent concentration at the front, c_1^0, was determined from knowledge of the glass transition temperature of the dry substance, as described by Fujita and Kishimoto [14]:

$$c^* = \frac{T_g - T}{\beta/\alpha_f} \tag{13}$$

Here, T_g was the glass transition temperature, T was the experimental temperature, b was a constant representative of the specific polymer/solvent system which can be determined by stress-relaxation experiments and the WLF equation [15], and α_f was the free volume constant of the dry polymer. Values of α_f and β have been tabulated for a variety of polymer systems [15].

Appropriate boundary conditions and initial conditions were used, assuming a uniform initial drug concentration in a completely dry polymer. Symmetry conditions were also used for solution of Eq. (11).

$$t = 0 \quad -\delta < x < \delta \quad c_1 = 0 \tag{14}$$

$$x = 0 \quad t > 0 \quad \frac{\partial c_1}{\partial x} = 0 \tag{15}$$

$$x = \pm\delta \quad t > 0 \quad c_1 = c_{1e} \tag{16}$$

Due to the partitioning effect at the surface of the gel (viz., Fig. 2), the surface boundary condition (Eq. (16)) was modified using an appropriate equation representing the time-dependence of the surface solvent concentration. At the interface between the swelling region of the polymer and pure water, a partition coefficient described the ratio of bulk water concentration to the equilibrium water concentration, $c_{1,e}$, in the swollen gel ($c_{1,e} = Kc_1^0$). Furthermore, the approach of the water concentration to its equilibrium value was assumed to occur as a time dependent function,

$$\{x = \pm\delta \quad t > 0 \quad c_1 = c_{1,e}(1 - e^{-t/\lambda}) \tag{17}$$

In this equation, λ represented the characteristic relaxation time for the polymer. For large values of λ, the swelling polymer reached its equilibrium state only after a long period of time. However, for small λ the concentration reached equilibrium almost immediately upon solvent penetration. This boundary condition was modified to include the diffusional Deborah number as well:

$$x = \pm\delta \quad t > 0 \quad c_1 = c_{1,e}\left(1 - \exp\left[\frac{-D_{1,2}t}{De(\delta_r)^2}\right]\right) \tag{18}$$

Here, δ_r (the gel layer thickness) could be written as $\delta(t) - \delta_g(t)$, where $\delta(t)$ was the distance from the gel/water interface to the center of the hydrogel, and $\delta_g(t)$ was the distance from the center of the hydrogel to the interface between glassy and rubbery regions of the material.

Before proceeding to a determination of solute transport, the solvent penetration equation must be solved first for $c_1(x,t)$ so that a drug release profile, as extracted from $c_3(x,t)$, could be constructed.

4. Development of mathematical model for drug transport

Solute release was modeled as a Fickian diffusion problem, with non-Fickian behavior introduced through the dependence of drug concentrations, c_3,on solvent uptake, c_1.

$$\frac{\partial c_3}{\partial t} = \frac{\partial}{\partial x}\left\{D_{3,2}\frac{\partial c_3}{\partial x}\right\} \tag{19}$$

The concentration dependence of the drug diffusion coefficient was also assumed to follow the Fujita expression:

$$D_{3,2} = D_3^0 \exp\left[-\beta_3\left(1 - \frac{c_1}{c_{1e}}\right)\right] \tag{20}$$

The drug diffusivity was seen to be strongly dependent on the concentration of water in the rubbery or glassy layer. From Eq. (20), the limit of $D_{3,2}$ as the hydrogel reached equilibrium was the drug diffusivity in the swollen polymer, D_3^0. β_3 is a material constant, as above, with typical values between 2 and 4.

Initial and boundary conditions similar to those used for determining water concentrations were used for this problem. A perfect sink condition ($c_3 = 0$) was used to describe the boundary at the surface of the polymer sample.

$$t = 0 \quad -\delta < x < \delta \quad c_3 = c_3^0 \tag{21}$$

$$x = 0 \quad t > 0 \quad \frac{\partial c_3}{\partial x} = 0 \tag{22}$$

$$x = \pm d \quad t > 0 \quad c_3 = 0 \tag{23}$$

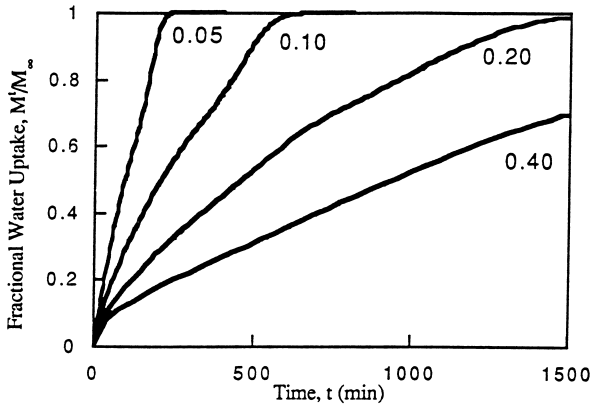

Fig. 3. Effect of sample thickness on water uptake into crosslinked polymers, as determined by the mathematical model developed in this work. Sample thicknesses are listed in cm next to each curve. The water diffusion coefficient used was 5×10^{-7} cm^2/s, characteristic polymer relaxation time was 20 min, and the water front velocity was 2×10^{-6} cm/s.

Accumulation of drug in the solution surrounding the sample was assumed to have a negligible effect on the transport process, which was an appropriate assumption, for at least the first 90% of a typical release experiment. This assumption held true as long as c_3 at $x = \delta$ is significantly greater than the concentration in the release medium (and since release experiments were conducted using polymer samples with volumes less than 0.1 ml compared with a release volume of at least 200 ml, this assumption was valid).

The two partial differential equations were non-dimensionalized to normalize parameters which varied slightly between experimental systems. The following dimensionless variables were defined for use in mathematical calculations

$$\text{Position}: \quad \zeta = \frac{x}{\delta_0} \tag{24}$$

$$\text{Time}: \quad \tau = \frac{D_1^0 t}{\delta_0^2} \tag{25}$$

$$\text{Solvent concentration}: \quad \psi_1(\zeta, \tau) = \frac{c_1}{c_{1e}} \tag{26}$$

$$\text{Solute concentration}: \quad \psi_3(\zeta, \tau) = 1 - \frac{c_3}{c_3^0} \tag{27}$$

These variables were designed such that ζ ranged from -1 to 1 between the polymer surfaces, and τ was a Fourier time. The term ψ_1 started with a value of 0, increasing to 1 as water was absorbed to its equilibrium concentration, c_{1e}. The term ψ_3 also increased from 0 to 1 during the swelling-controlled release process.

The mathematical problem was solved numerically, using forward time-centered space finite divided differences [16] to determine first $c_1(x,t)$ and then $c_3(x,t)$. A computer program was written in FORTRAN and executed on a VAX 3090 using 600 000 time interval steps across 20 position elements. Diffusivities at each of the position elements were assigned relative to the calculated swelling front. Truncation errors were on the order of the square of the time step interval.

5. Water sorption and drug release results from mathematical models

With appropriate assumptions and the numerical analysis procedures described previously, the partial differential equations representing the coupling of diffusional and relaxation processes were solved to yield the normalized water and drug concentrations in the polymer slab as functions of position and time. These results were then integrated to yield fractional water uptake and fractional release plots. The computer program was run for a range of Swelling Interface and diffusional Deborah numbers to achieve a graphical representation of how molecular factors impacted the sorption and drug release profiles. It was attempted to maintain as many system parameters constant in comparing the effects of *Sw* and *De* on release. Experimental data from the same laboratory [17,18] were used in comparisons between model predictions and swelling and release profiles. The effects of molecular factors, such as solute molecular weight and hydrophilicity, crosslinking ratio, and polymer composition are detailed in these papers.

5.1. Water sorption

The effects of sample thickness, front velocity, characteristic stress relaxation time and water diffusion coefficients were investigated (Figs. 3–6) by comparison of three different parameter values to a base case. The base case, identified as trial A in Table 1, used the following model parameters: a sample thickness of 0.10 cm, water diffusion coefficient of

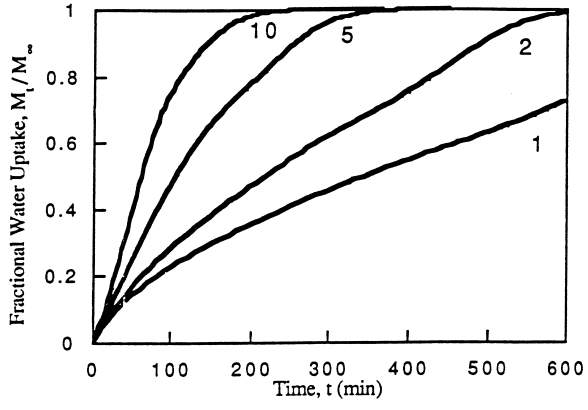

Fig. 4. Effect of front velocity on water uptake into crosslinked polymers, as determined by the mathematical model developed in this work. Front velocities are listed in the figure, $\times 10^{-6}$ cm/s. The water diffusion coefficient used was 5×10^{-7} cm^2/s, characteristic polymer relaxation time was 20 min, and the sample thickness was 0.1 cm.

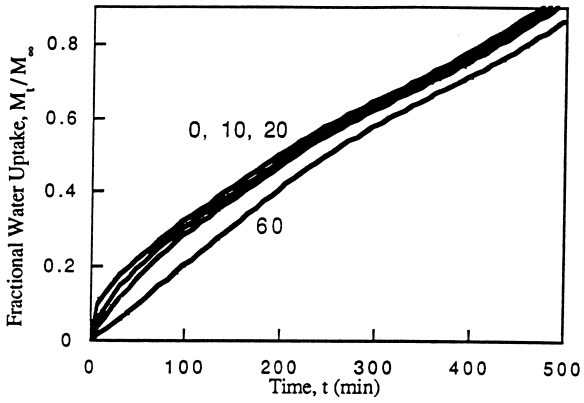

Fig. 5. Effect of polymer relaxation time, λ, on water uptake into crosslinked polymers, as determined by the mathematical model developed in this work. Relaxation times were 0, 10, 20 and 60 min, from left to right on the figure. The water diffusion coefficient used was 5×10^{-7} cm^2/s, front velocity was 2×10^{-6} cm/s, and the sample thickness was 0.1 cm.

5×10^{-7} cm^2/s, characteristic polymer relaxation time of 20 min, and a front velocity of 2×10^{-6} cm/s.

As seen in Fig. 3, the thickness of a polymer sample, δ, through which water penetrates during the sorption process, has an impact on water uptake profiles. For processes having the same water diffusion coefficient, polymer relaxation time, and front velocity, an increase in sample thickness from 0.05 to 0.40 cm increased the length of time required for the polymer to absorb water to reach equilibrium from 300 to nearly 2000 min (Fig. 3). The effect of sample thickness on diffusional exponent, n, for water sorption was also investigated, and values were tabulated in Table 1. Simulations were conducted for sample thicknesses ranging from 0.05 to 0.40 cm (trials A, B, C and D), with the resulting n values ranging from 0.69 to 0.73, with higher n values, due to polymer relaxation dominating Fickian transport, observed in the thinner samples.

Water diffusion in polymers promotes a front velocity

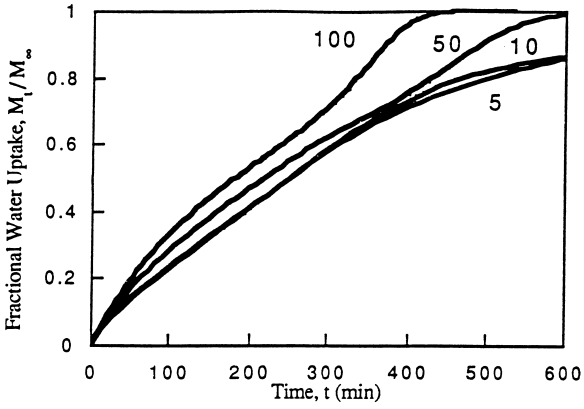

Fig. 6. Effect of water diffusion coefficient, $D_{1,2}$, on water uptake into crosslinked polymers, as determined by the mathematical model developed in this work. Water diffusion coefficients are listed in the figure $\times 10^{-8}$ cm^2/s. The front velocity used was 2×10^{-6} cm/s, characteristic polymer relaxation time was 20 min, and the sample thickness was 0.1 cm.

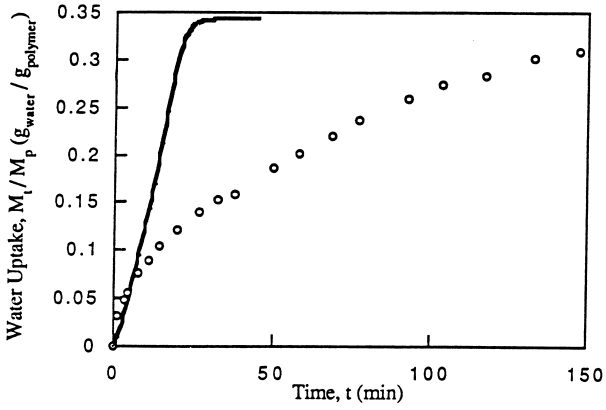

Fig. 7. Comparison of model prediction vs. experimental data for water uptake in p(HEMA-co-MMA) hydrogels containing 75 mol% HEMA formed by thermal initiation with a nominal crosslinking ratio of 0.01.

related to stresses occurring during sorption. When front velocities, v, were varied in the model from 1 to 10×10^{-6} cm/s, while holding all other variables constant, the water transport obeyed the power law model, with n values ranging from 0.63 to 1.01 (Table 1). Case II transport was observed for the highest front velocity, 10.0×10^{-6} cm/s, as indicated in Fig. 4.

Characteristic polymer relaxation times were incorporated into the mathematical model to account for polymer rearrangement during sorption, and had only a minor effect on water uptake profiles, at least in the range of λ values investigated. As polymer relaxation times increased from 0 to 60 min, the rate of sorption decreased slightly, as shown in Fig. 5. Higher λ values caused greater deviation from Fickian transport behavior, with diffusional exponents increasing from 0.58 to 0.79 as relaxation times increased from 0 to 60 min (Table 1).

The final variable investigated in the mathematical diffusion model was the diffusion coefficient of water. In experimental systems, this diffusion coefficient was greatly influenced by the presence of the hydrogel mesh, therefore water uptake profiles reported from the mathematical calcu-

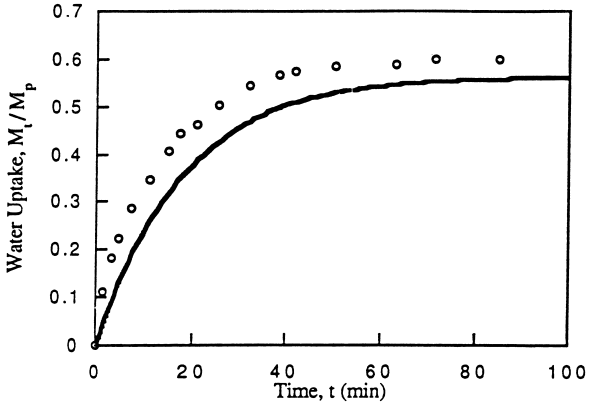

Fig. 8. Comparison of model prediction vs. experimental data for water uptake in crosslinked PHEMA samples formed by thermal initiation with a nominal crosslinking ratio of 0.01.

Table 1
Diffusional exponents, n, and diffusional Deborah numbers, De, for water uptake in systems determined from mathematical model

Trial	Thickness, δ (cm)	Front velocity, v ($\times 10^6$ cm/s)	Stress relaxation, l (min)	Water diffusion coefficient, $D_{1,2}$ ($\times 10^8$ cm^2/s)	Diffusional exponent, n	Diffusional Deborah No., De
A	0.10	2.0	20	50.0	0.728	0.24
B	0.05	2.0	20	50.0	0.716	0.96
C	0.20	2.0	20	50.0	0.693	0.06
D	0.40	2.0	20	50.0	0.693	0.015
E	0.10	10.0	20	50.0	1.015	0.24
F	0.10	5.0	20	50.0	0.789	0.24
G	0.10	1.0	20	50.0	0.628	0.24
H	0.10	2.0	60	50.0	0.791	0.72
I	0.10	2.0	10	50.0	0.656	0.12
J	0.10	2.0	0	50.0	0.585	0.00
K	0.10	2.0	20	5.0	0.831	0.024
L	0.10	2.0	20	10.0	0.803	0.048
M	0.10	2.0	20	100.0	0.712	0.48

lations displayed some variation due to changes in $D_{1,2}$ values. The system with the highest $D_{1,2}$ value had the fastest sorption rate, while nearly limiting diffusion coefficients were reached for $D_{1,2} = 1 \times 10^{-7}$ and 5×10^{-8} cm^2/s, with little difference in the swelling profiles. This was attributed to the greater influence of the convective diffusion term as the Fickian diffusion term decreased in value with $D_{1,2}$. For low water diffusion coefficients, diffusional exponents (Table 1) were higher indicating that polymer relaxation processes dominate the sorption process, especially for samples K and L.

Using diffusion coefficients reported in literature, model parameters characteristic of each polymer system and the relaxation times reported in this work, water uptake profiles were determined by the computer program and compared to experimental results. The same sample thicknesses were used in the model as those measured for each swelling experiment. Results are shown for water sorption into P(HEMA-co-MMA) and PVA hydrogels in Figs. 7–11. Because moving boundary conditions were not employed in the model to account for sample thickness increases during sorption, some of the model results do not compare well with the experimental data, especially for the PVA systems where expansion of the polymer was significant.

In Fig. 8, the model prediction for water uptake into crosslinked PHEMA samples shows nearly the same profile as that recorded experimentally, with the sorption process occurring over about 50 min. The model-predicted curve slightly lags the experimental data; this was attributed to an increase in the influence of the convective term at initial times during the sorption experiment, and the possibility that osmotic forces may increase water uptake slightly.

In Fig. 10, the dual sorption behavior observed in the experimental data was predicted by the model, as shown by the increase in water uptake about 100 min into the swelling process.

5.2. Drug release

Simulations using the mathematical model were used to determine fractional solute release as a function of sample thickness, δ (Fig. 12), water diffusion coefficient, $D_{1,2}$ (Fig. 13), drug diffusion coefficient, $D_{3,21}$ (Fig. 14), and front velocity, v (Fig. 15). Using the power law model (Eq. (3)) to fit release data, values of n were tabulated for each simulation (Table 2).Diffusional Deborah and Swelling Interface numbers were determined based on parameters used in the simulations and are also listed in Table 2. The base case for all comparisons was trial N, with a sample having a dry thickness of 0.20 cm, a front velocity of 2.0×10^{-6} cm/s, stress relaxation time of 20 min, and water and drug diffusion coefficients of 5×10^{-7} and 5×10^{-6} cm^2/s, respectively.

Computer simulations were carried out for sample thicknesses ranging from 0.05 to 0.40 cm. Case II-type transport was observed for the thinnest sample, trial O in Table 2 All of the drug was released in less than 500 min (Fig. 12) for this thickness, and the diffusional exponent was 0.71, with a corresponding diffusional Deborah number of 0.96 and a Swelling Interface number of 0.02. As the sample thickness was increased, solute release slowed, and n values decreased to 0.63, with more Fickian-type transport observed for a 0.40 cm thick sample.

Changes in the water diffusion coefficient through the gel had a slightly smaller effect on transport behavior than sample thickness. In Fig. 13, the highest water diffusion coefficient, 1×10^{-6} cm^2/s, led to the fastest solute release, with all drug being exhausted after 3000 min, compared to drug release times greater than 5000 min for $D_{1,2}$ values of 5×10^{-7} cm^2/s or less. Super Case II transport was observed in two of the cases, with drug being liberated more freely when water penetrated the sample completely. There was little difference in drug release profiles for $D_{1,2}$ values of 10 and 5×10^{-8} cm^2/s. Diffusional exponent, n, values

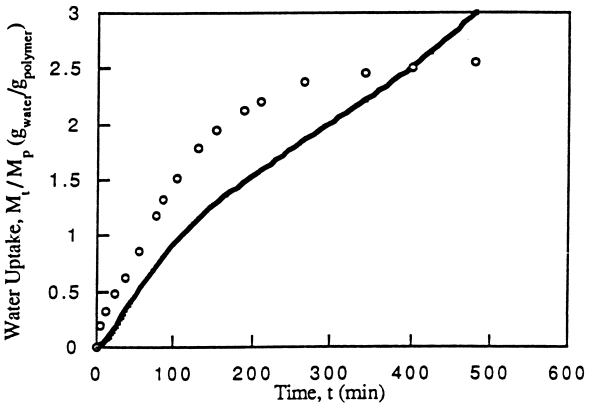

Fig. 9. Comparison of model prediction vs. experimental data for water uptake in PVA hydrogels formed from a 15 wt.% aqueous PVA solution with initial $\bar{M}_n = 48\,200$, and having a 99% degree of hydrolysis. The nominal crosslinking ratio was 0.01

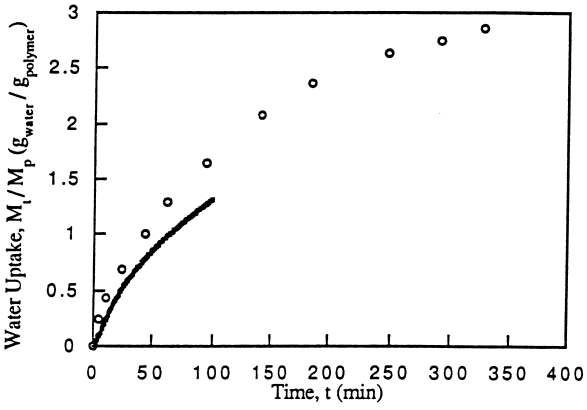

Fig. 11. Comparison of model prediction vs. experimental data for water uptake in PVA hydrogels formed from a 15 wt.% aqueous PVA solution with initial $\bar{M}_n = 15\,800$, and having an 85% degree of hydrolysis. The nominal crosslinking ratio was 0.01.

decreased from 0.67 to 0.57 (Table 2) with increasing water diffusion coefficients, indicating that Fickian solute transport dominated for small water diffusion coefficients.

Solute release profiles as a function of the drug diffusion coefficient, $D_{3,21}$, were plotted in Fig. 14. Fastest release occurred for the highest diffusion coefficient, $D_{3,21} = 1 \times 10^{-5}$ cm^2/s, trial W. The highest n value, 0.75, observed for this set of data was for trial V, with a drug diffusion coefficient of 5×10^{-7} cm^2/s, and n values decreased with increasing drug diffusion coefficients to a minimum of 0.61.

The final model parameter which was varied to observe the effect on solute release was the water front velocity (Fig. 15). For the four velocity values chosen, three of the drug release curves collapsed into a single curve. These three front velocities were 20, 50 and 100×10^{-7} cm/s, while the rate of drug release was diminished for a front velocity of 5×10^{-7} cm/s. The drug release diffusional exponent was 0.635 for the three higher front velocities, while $n = 0.744$ for the lower front velocity. This difference was attributed to the decrease in the rate of water sorption, which decreased the Fickian component of drug diffusion, while the same drug release profile observed for three different front velocities indicated a cut-off value of v, beyond which drug release was limited by other parameters.

Drug release profiles were generated from the mathematical model using diffusion coefficients for water and drugs reported in literature, and polymer parameters according to the experimental sample. Again, sample thicknesses used in the computer program matched those of experimental measurements. A few polymer/drug systems for which enough data were available were selected for use in the mathematical model. These systems included the release of theophylline, triamterene and vitamin B_{12} from P(HEMA-co-MMA) and PVA hydrogels. Comparison of experimental results to model predictions in many cases did not show good correlation. This was attributed to the assumption in the model that the sample thickness remains

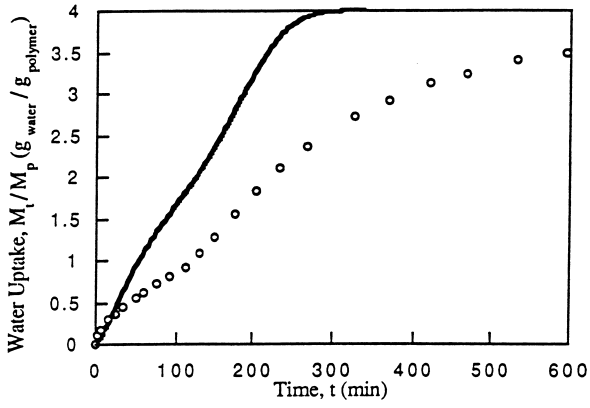

Fig. 10. Comparison of model prediction vs. experimental data for water uptake in PVA hydrogels formed from a 15 wt.% aqueous PVA solution with initial $\bar{M}_n = 35\,700$, and having a 99% degree of hydrolysis. The nominal crosslinking ratio was 0.01.

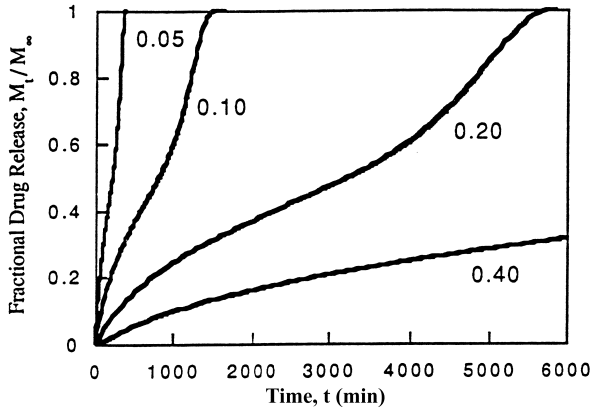

Fig. 12. Effect of sample thickness, δ, on drug release from crosslinked polymers, as determined by the mathematical model developed in this work. Sample thicknesses are listed in cm. The front velocity used was 2×10^{-6} cm/s, characteristic polymer relaxation time was 20 min, the drug diffusion coefficient was 5×10^{-6} cm^2/s, and the water diffusion coefficient was 5×10^{-7} cm^2/s.

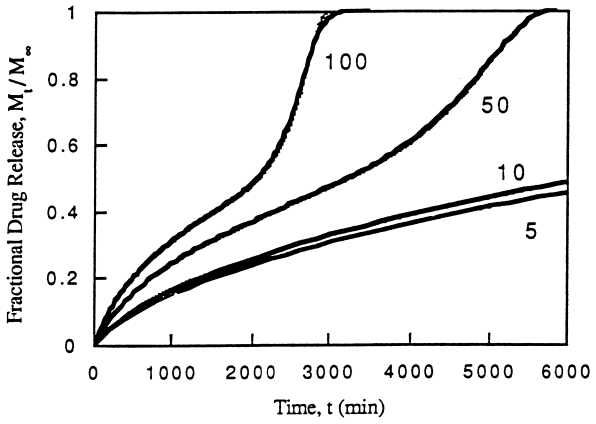

Fig. 13. Effect of water diffusion coefficient, $D_{1,2}$, on drug release from crosslinked polymers, as determined by the mathematical model developed in this work. Water diffusion coefficients are listed in the figure $\times 10^{-8}$ cm^2/s. The front velocity used was 2×10^{-6} cm/s, characteristic polymer relaxation time was 20 min, and the sample thickness was 0.20 cm.

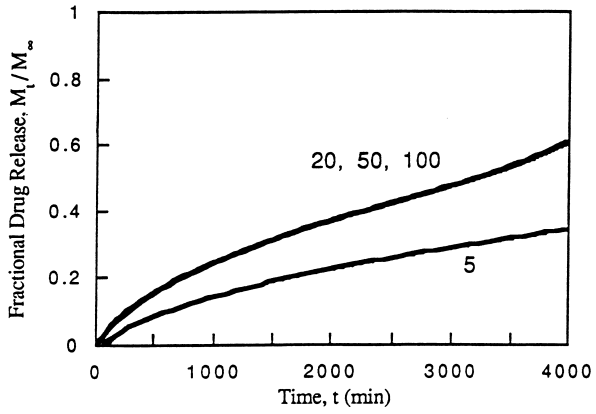

Fig. 15. Effect of front velocity, v, on drug release from crosslinked polymers, as determined by the mathematical model developed in this work. Front velocities are listed in the figure $\times 10^{-7}$ cm/s. The characteristic polymer relaxation time was 20 min, the sample thickness was 0.20 cm, the drug diffusion coefficient was 5×10^{-6} cm^2/s, and the water diffusion coefficient was 5×10^{-7} cm^2/s.

constant during the swelling process, and was a particularly bad assumption for the crosslinked PVA systems.

Fractional drug release is shown as a function of time for experimental data and model predicted profiles in Figs. 15–19. In general, the model was able to predict the time scale of the drug release, although there was some deviation from experimental data, especially due to factors not included in the model, such as drug hydrophilicity and the possibility of diffusion hindrance due to trapping of drug molecules during release.

Theophylline release from three experimental systems were plotted as a function of time, against the model predictions. Theophylline release was predicted well by the model in Fig. 16, for release from a PVA hydrogel formed from chains with an initial molecular weight of 35 700. The rapid release of theophylline from the most hydrophilic PVA gel was also predicted by the model, with the majority of release occurring during the first 5 min of the experiment.

Triamterene release from two PVA hydrogel systems was compared to release profiles generated by the computer model, with results shown in Fig. 17. The model predicted faster release times than in either of the experimental systems, but this was attributed to the relative hydrophobicity of triamterene, which decreased the release rates from those predicted from diffusion coefficients in free solution.

The final drug used in model-generated release profiles was vitamin B_{12}. Release of vitamin B_{12} was plotted against model predictions for four polymer carriers. The extremely slow release rates observed for vitamin B12 release from P(HEMA-co-MMA) hydrogels containing 75 mol% HEMA was predicted well by the model, as shown in Fig. 8. Dual-sorptive-type release behavior was predicted for vitamin B12 release from PHEMA and PVA hydrogels in Fig. 19,

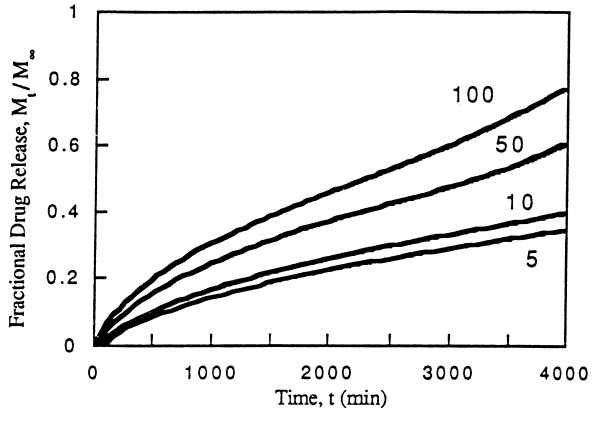

Fig. 14. Effect of drug diffusion coefficient, $D_{3,21}$, on drug release from crosslinked polymers, as determined by the mathematical model developed in this work. Drug diffusion coefficients are listed in the figure $\times 10^{-7}$ cm^2/s. The front velocity used was 2×10^{-6} cm/s, characteristic polymer relaxation time was 20 min, the sample thickness was 0.20 cm, and the water diffusion coefficient was 5×10^{-7} cm^2/s.

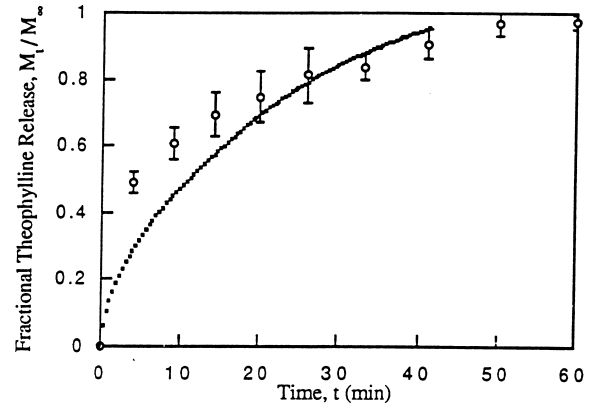

Fig. 16. Comparison of model prediction vs. experimental data for theophylline release from PVA hydrogels formed from a 15 wt.% aqueous PVA solution with initial $\bar{M}_n = 35\,700$, and having a 99% degree of hydrolysis. The nominal crosslinking ratio was 0.01. Drug was loaded by equilibrium partitioning from a concentrated aqueous solution for 14 days.

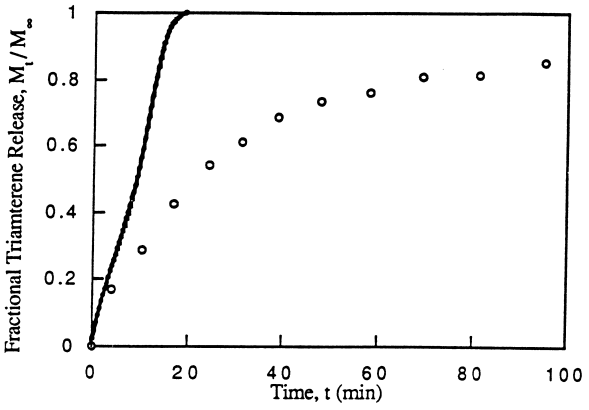

Fig. 17. Comparison of model prediction vs. experimental data for triamterene release from PVA hydrogels formed from a 15 wt.% aqueous PVA solution with initial $\bar{M}_n = 48\,200$, and having a 99% degree of hydrolysis. The nominal crosslinking ratio was 0.01. Drug was loaded by equilibrium partitioning from a concentrated aqueous solution for 14 days.

although the time scale of release was predicted relatively well for each case, with release occurring over 10 000, 200 and 70 min for each case.

Experimental verification of the model was carried out as well by comparison of the model-generated release profiles to experimental data. *De* and *Sw* were determined for each experimental system, and compared to the model predictions. Many of the same trends were seen in the experimental studies as the model simulations of water and drug diffusion, although some differences were attributed to the lack of incorporation in the model of moving boundaries due to changes in sample thickness

Diffusional Deborah numbers for the simulations of water uptake were plotted as a function of the sorption diffusion exponent, *n*, in Fig. 20. A trend in this data was hard to discern, but there was a general decrease in diffusional Deborah numbers with increasing water sorption *n* values.

Swelling Interface numbers were plotted in Fig. 21 as a

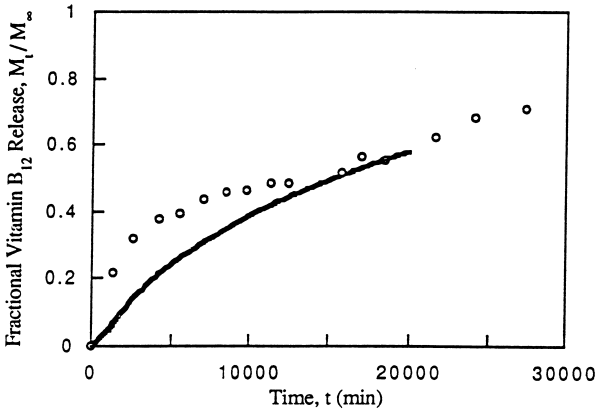

Fig. 18. Comparison of model prediction vs. experimental data for vitamin B_{12} release from P(HEMA-co-MMA) hydrogels containing 75 mol% HEMA formed by thermal initiation with a nominal crosslinking ratio of 0.01. Drug was loaded by equilibrium partitioning from a concentrated aqueous solution for 14 days.

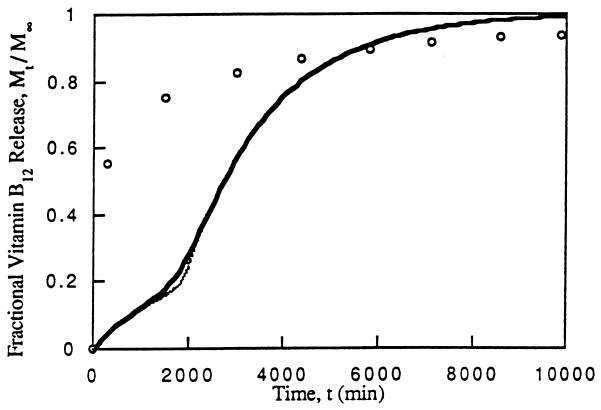

Fig. 19. Comparison of model prediction vs. experimental data for vitamin B_{12} release from PHEMA hydrogels formed by thermal initiation with a nominal crosslinking ratio of 0.01. Drug was loaded by equilibrium partitioning from a concentrated aqueous solution for 14 days.

function of the drug release diffusion exponent, *n*. The trends observed here are opposite, with *Sw* values decreasing with increasing *n* for simulations.

6. Conclusions

Prediction of release profiles from molecular and geometrical information showed the effects of sample thickness, water and drug diffusion coefficients and polymer viscoelastic response (viz. relaxation time) on the resulting swelling and release profiles. The information gleaned from the model show that the swelling profile is markedly changed with relatively small changes in sample thickness, especially when compared to the results observed for differences in polymer relaxation time. The model developed in this work provides a graphic depiction of the correlation between and relative importance of molecular factors in designing a controlled release system. The model can be improved upon to more accurately predict experimental systems through the use of moving boundaries to simulate the swelling behavior, and a better understanding of diffu-

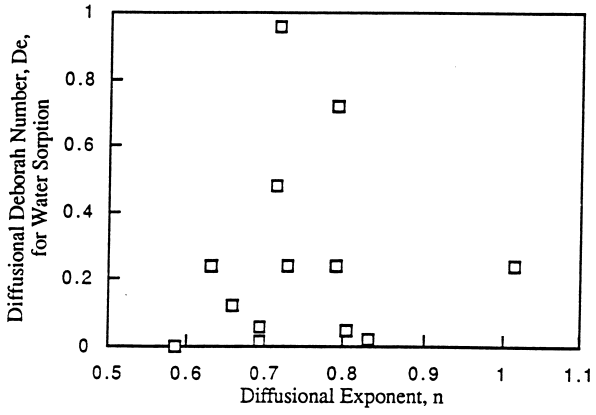

Fig. 20. Diffusional Deborah numbers, *De*, as determined from mathematical model, as a function of diffusional exponents for water uptake.

Table 2
Diffusional exponents, n, diffusional Deborah numbers, De, and swelling interface numbers, Sw, for water uptake in systems determined from mathematical model

Trial	Thickness, δ (cm)	Front velocity, υ ($\times 10^6$ cm/s)	Stress relaxation λ (min)	Water diffusion coefficient, $D_{1,2}$ ($\times 10^8$ cm^2/s)	Drug diffusion coefficient, $D_{3,21}$ ($\times 10^7$ cm^2/s)	Diffusional exponent, n	Diffusional Deborah number, De	Swelling interface number, Sw
N	0.20	2.0	20	50.0	50.0	0.635	0.06	0.08
O	0.05	2.0	20	50.0	50.0	0.710	0.96	0.02
P	0.10	2.0	20	50.0	50.0	0.659	0.24	0.04
Q	0.40	2.0	20	50.0	50.0	0.636	0.015	0.16
R	0.20	2.0	20	100.0	50.0	0.672	0.12	0.08
S	0.20	2.0	20	10.0	50.0	0.582	0.012	0.08
T	0.20	2.0	20	5.0	50.0	0.571	0.006	0.08
U	0.20	2.0	20	50.0	10.0	0.707	0.06	0.40
V	0.20	2.0	20	50.0	5.0	0.746	0.06	0.80
W	0.20	2.0	20	50.0	100.0	0.612	0.06	0.04
X	0.20	10.0	20	50.0	50.0	0.635	0.06	0.40
Y	0.20	5.0	20	50.0	50.0	0.635	0.06	0.20
Z	0.20	0.5	20	50.0	50.0	0.744	0.06	0.02

sive behavior of the solutes imbedded in polymer networks.

7. Nomenclature for mathematical modeling equations

7.1. Roman symbols

c_1, concentration of water (function of position and time)
$c_{1,e}$, equilibrium water concentration in polymer gel
c_2, concentration of polymer
c_3, concentration of drug
c_1^0, initial (constant) water concentration outside of gel
c_3^0, initial drug concentration inside polymer
c_1^*, critical concentration observed at the boundary between glassy and rubbery regions
$D_{1,2}$, diffusion coefficient of water through polymer
D_1^0, diffusion coefficient of water through the swollen gel
$D_{3,2}$, diffusion coefficient of drug through gel

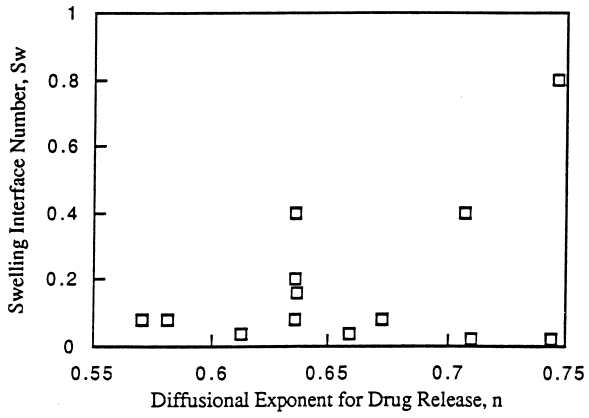

Fig. 21. Swelling interface numbers, Sw, as determined from mathematical model, as a function of diffusional exponents for drug release.

D_3^0, diffusion coefficient of drug in the swollen gel
K, partition coefficient of water between solution and gel phases
l, length of sample surface exposed to penetrating solvent
t, time
T, experimental temperature
T_g, glass transition temperature
x, position
Sw, Swelling interface number
De, Diffusional Deborah number

7.2. Greek symbols

α_f, dry polymer free volume constant
β, a constant characteristic of the polymer/water system
β_1, free volume material constant related to water diffusivity
β_3, free volume material constant related to water diffusivity
δ_r, gel (rubbery) layer thickness
δ_g, glassy layer thickness
δ_0, initial half-thickness of sample
ζ, dimensionless position
θ, characteristic diffusion time for water in polymer
λ, characteristic relaxation time
τ, dimensionless time
υ, swelling front velocity
ψ_1, dimensionless water concentration (c_1/c_1^0)
ψ_3, dimensionless water concentration (c_3/c_3^0)

Acknowledgements

This work was supported in part by grants from the National Science Foundation and the Showalter Trust.

References

[1] R.W. Korsmeyer, S.R. Lustig, N.A. Peppas, Solute and penetrant diffusion in swellable polymers. I. Mathematical modeling, J. Polym. Sci. B Polym. Phys. 24 (1986) 395–408.

[2] S.R. Lustig, N.A. Peppas, Solute and penetrant diffusion in swellable polymers. VII. A free volume-based model with mechanical relaxation, J. Appl. Polym. Sci. 33 (1987) 533–549.

[3] J.H. Petropoulos, K.G. Papadokostaki, S.G. Amarantos, A general model for the release of active agents incorporated in swellable polymeric matrices, J. Polym. Sci. B Polym. Phys. 30 (1992) 717–725.

[4] P.I. Lee, Diffusional release of a solute from a polymeric matrix – approximate analytical solutions, J. Membr. Sci. 7 (1980) 255–275.

[5] S. Joshi, G. Astarita, Mathematical model of the desorption of swelling solvents from swollen polymer films, Polymer 20 (1979) 1217–1220.

[6] J.C. Wu, N.A. Peppas, Modeling of penetrant diffusion in glassy polymers with an integral sorption Deborah number, J. Polym. Sci. B Polym. Phys. 31 (1993) 1503–1518.

[7] J. Klier, N.A. Peppas, Solute and penetrant diffusion in swellable polymers. VIII. Influence of the swelling interface number on solute concentration profiles and release, J. Control. Release 7 (1988) 61–68.

[8] N.A. Peppas, N.M. Franson, The swelling interface number as a criterion for prediction of diffusional solute release mechanisms in swellable polymers, J. Polym. Sci. Polym. Phys. 21 (1983) 983–997.

[9] J.S. Vrentas, C.M. Jarzebski, J.L. Duda, A Deborah number for diffusion in polymer-solvent systems, AIChE J. 21 (1975) 894–901.

[10] G. Astarita, G. Marucci, Principles of Non-Newtonian Fluid Mechanics, McGraw-Hill, London, 1974.

[11] P.L. Ritger, N.A. Peppas, A simple equation for description of solute release. I. Fickian and non-fickian release from non-swellable devices in the form of slabs, spheres, cylinders or discs, J. Control. Release 5 (1987) 23–36.

[12] H.B. Hopfenberg, H.L. Frisch, Transport of organic micromolecules in amorphous polymers, J. Polym. Sci. Polym. Lett. 7 (1969) 405–409.

[13] H. Fujita, Polymer diluent systems, Forsch. Hochpolym. Forsch. 3 (1961) 1–41.

[14] H. Fujita, A. Kishimoto, Diffusion-controlled stress relaxation in polymers. II. Stress relaxation in swollen polymers, J. Polym. Sci. 28 (1958) 547–558.

[15] J.D. Ferry, Viscoelastic Properties of Polymers, 2, Wiley, New York, 1970.

[16] J.D. Hoffman, Numerical Methods for Egineers and Sientists, 1, McGraw-Hill, St. Louis, 1992.

[17] C.S. Brazel, N.A. Peppas, Mechanisms of solute and drug transport in relaxing, swellable, hydrophilic glassy polymers, Polymer 40 (1999) 3383–3398.

[18] C.S. Brazel, N.A. Peppas, Dimensionless analysis of swelling of hydrophilic glassy polymers with subsequent drug release from relaxing structures, Biomaterials 20 (1999) 721–732.